PERGAMON

Radiation Physics and Chemistry 65 (2002) 109–121

Radiation Physics and Chemistry

www.elsevier.com/locate/radphyschem

# Near K-edge linear attenuation coefficients for Si, $SiO_2$ and $Si_3N_4$

Alan Owens[a,*], G.W. Fraser[b], S.J. Gurman[b]

[a] *Science Payloads Technology Division, ESA/ESTEC, Postbus 299, 2200AG Noordwijk, Netherlands*
[b] *Department of Physics and Astronomy, Leicester University, Leicester LE1 7RH, UK*

Received 19 October 2001; accepted 7 January 2002

**Abstract**

We present tabulated near K-edge linear attenuation coefficients for a range of materials commonly used in MOS construction; namely, crystalline silicon (Si-c), amorphous silicon (Si-a), amorphous silicon dioxide ($SiO_2$-a) and amorphous silicon nitride ($Si_3N_4$-a). The coefficients were derived from total photocurrent measurements of X-ray absorption fine structure (XAFS) obtained at the Daresbury Synchrotron Radiation Source and show considerable near-edge structure when compared to curves generated from standard atomic data tables. 

## 1. Introduction

The present generation of large area X-ray detectors based on silicon charge coupled technologies have sufficiently high spectroscopic resolutions to begin to resolve internally induced structure in their photo response (e.g., see Owens et al., 1996, 1997a). This structure is due to the energy dependence of the X-ray absorption coefficients of the materials of which the device is constructed. It is particularly strong for energies close to absorption edges and in these regions reflects the X-ray absorption fine structure (XAFS). Recent work (Owens et al., 1996; Prigozhin et al., 1998) with a front illuminated CCD has shown that XAFS in the photo response originates in surface features of the device (i.e., electrodes, gate dielectrics, polysilicon gates and passivation layers). It arises from interference effects generated due to the escaping photoelectrons following X-ray absorption and is produced in the first few microns of surface (see Gurman, 1990). Since the dimensions of the surface features encountered in MOS construction are of the same order, this has led to the surprising conclusion that the response of a CCD near its absorption edges is dominated by its surface chemistry instead of the bulk properties of the device (Owens, 2002). The increasing use of silicon detectors (for example in X-ray astronomy) to search for spectral features at or around the absorption edges of the constituent materials has produced an urgent need for a tabulated set of linear attenuation coefficients that incorporate the effects of XAFS. Unfortunately, tables published to date represent the unperturbed atomic cross sections for isolated atoms, which do not consider the collective properties of an ensemble. As such, it is not possible to use them to accurately model device responses around the absorption edges. Since a search of the literature failed to produce the necessary tables, we have derived near-edge linear attenuation coefficients from total photocurrent measurements of test samples obtained at a synchrotron radiation facility. Data are given for a variety of materials commonly used in MOS construction—crystalline silicon (Si-c), amorphous silicon (Si-a), amorphous silicon dioxide ($SiO_2$-a) and amorphous silicon nitride ($Si_3N_4$-a). It is important to note that while an infinite degree of crystallinity can exist, the specific samples tested were chosen to be representative of their class. The general trends with energy follow standard calculations, such as Cromer and

*Corresponding author. Tel.: +31-71-565-5326; fax: +31-71-565-4690.
*E-mail address:* aowens@rssd.esa.int (A. Owens).

0969-806X/02/$ - see front matter 
PII: S0969-806X(02)00207-4

Liberman (1970), but show considerable structure above the edge. It is important to note that these measurements can only be made at a synchrotron radiation facility, since the separation between calibration lines used in traditional techniques using discrete X-ray lines is much greater than the characteristic XAFS energy scale.

## 2. Experimental

Total photo-yields were measured on the SOXAFS beam-line, station 3.4 (Roper et al., 1992), at the Daresbury Synchrotron Radiation Source (SRS). The experimental arrangement is shown in Fig 1. A beam from the synchrotron was extracted by bending magnet 3 and reflected off a chromium-coated flat onto a toroidal mirror. The mirror focused it onto a double crystal monochromator providing a collimated monochromatic beam at the sample. The crystals used for the present experiment were InSb(III). The flat downstream filters hard X-rays by grazing angle reflectivity to give a high-energy cut-off, ensuring that the spectrum at the sample is not contaminated by higher harmonics of the Bragg reflection. The incident beam intensity was determined by measuring the replacement current in a 0.25 μm thick aluminium foil placed into the beam between the sample and monochromator. The samples had dimensions $2\,\mathrm{cm} \times 1\,\mathrm{cm} \times 10^{-3}\,\mathrm{cm}$ and were mounted on a 1 mm thick copper substrate, which provided the electrical and mechanical interface. The monochromator was scanned from 1750 to $\sim$2500 eV in step sizes of 5 eV from 1750 to 1830 eV; 0.5 eV steps from 1830 to 1870 eV and 2 eV steps thereafter. At each energy setting the current drawn by the sample to maintain charge neutrality, $I_s$, was measured and logged, as was the current, $I_o$, in the beam intensity monitor. The electron drain current technique is standard practice at the SRS for soft X-ray measurements and is an adaptation of the commonly used total electron yield technique (Elam et al., 1988). Data taking was automatic, taking about 30 min to acquire each spectrum. To suppress statistical noise, three spectra were taken for each sample and averaged.

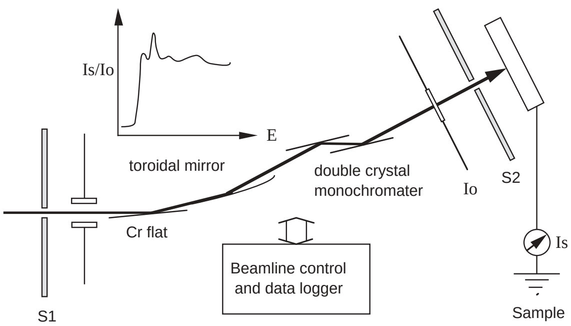


Fig. 1. The experimental configuration of beamline 3.4 at the Daresbury SRS.

## 3. Results

In Fig. 2 we show the total photocurrent, $\chi = I_s/I_o$, as a function of energy for all four samples. The data have been normalized to $I_o$ to correct for decay in synchrotron beam current and variations in intensity from the monochromator. Because of uncertainties in the monochromator setting, the dioxide and nitride curves have been displaced by 2 eV to give the correct relative distance from the silicon edge and all four curves adjusted so that the silicon edge falls at its accepted value of 1838.9 eV (Williams, 1986).

Recently, Cho et al. (1988) have argued that the observed XAFS must occur through indirect processes such as reabsorption of Auger electrons and fluorescent radiation. In fact, to first order, the total yield $\chi(E)$ is proportional to the product of the X-ray energy, $E$, and the absorption coefficient $\mu(E)$ (Henke et al., 1981). Thus, the drain current method gives a signal, which represents the detailed form of $\mu(E)$ modified by a smooth, slowly varying function of energy. This is the basis for its use as a detection method in X-ray absorption spectroscopy. For the present work, we have assumed the photo-yields, $\chi$, shown in Fig. 2 are related to the attenuation coefficients, $\mu$, by the function

$$\chi(E) = \mu(E)\{\alpha + \beta E\}. \tag{1}$$

The constants $\alpha$ and $\beta$ were determined by normalization at 1800 and 2300 eV to the calculations of Cromer and Liberman (1970) based on single atom absorption. The two bounds are not arbitrary but are

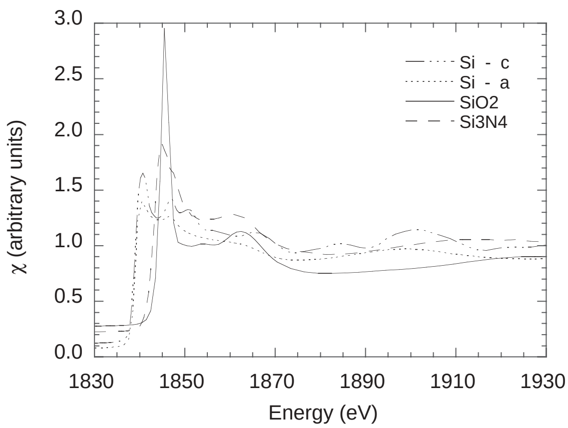


Fig. 2. Measured photocurrent X-ray absorption fine structure from a crystalline Si sample (c), an amorphous Si sample (a), an amorphous $SiO_2$ sample and an amorphous $Si_3N_4$ sample.

considered to be sufficiently above and below the edge to be free from structure. Eq. (1) was initially tested by comparing gold X-ray absorption coefficients derived from photocurrent measurements with the experimentally measured values of Veigele (1973). It was found that the expected relationship was accurate over the energy range 2200–3500 eV to a precision of a few percent (Owens et al., 1997b).

The derived linear attenuation coefficients for our samples are shown graphically in Fig. 3 along with the classical curve for Si predicted by Cromer and Liberman (1970). As expected, the amplitude of structure in amorphous silicon is reduced compared to the crystalline case. This is because in the transition from the crystalline to the amorphous phase in a covalent material like silicon, the disorder in bond angle generally suppresses the signal from atoms beyond the first coordination shell. The specific samples tested, had

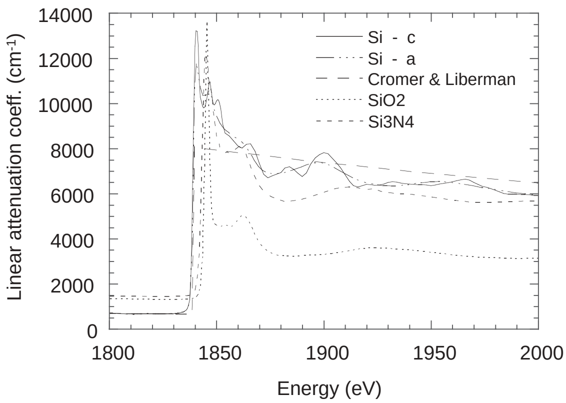


Fig. 3. The derived linear attenuation coefficients across the Si K-edge. For Si, the letters c and a refer to crystalline and amorphous. We also show the 'classical' Si curve based on the calculation of Cromer and Liberman (1970).

Table 1
Tabulated linear attenuation coefficients from 1800 to 2300 eV in 1 eV steps for crystalline silicon (Si-c), amorphous silicon (Si-a) amorphous silicon dioxide ($SiO_2$) and amorphous silicon nitride ($Si_3N_4$)

Linear attenuation coefficients ($cm^{-1}$)

| $E$ (eV) | Si-c | Si-a | $SiO_2$ | $Si_3N_4$ |
|---|---|---|---|---|
| 1800 | 706.0153 | 705.9860 | 1362.630 | 1468.180 |
| 1801 | 703.9272 | 706.3820 | 1360.650 | 1467.500 |
| 1802 | 701.8393 | 703.8380 | 1358.670 | 1466.820 |
| 1803 | 699.7565 | 698.3540 | 1356.690 | 1466.140 |
| 1804 | 697.7205 | 692.8700 | 1354.790 | 1465.350 |
| 1805 | 695.6844 | 687.3860 | 1352.970 | 1464.450 |
| 1806 | 693.6485 | 681.9020 | 1351.150 | 1463.550 |
| 1807 | 691.6125 | 677.0170 | 1349.330 | 1462.650 |
| 1808 | 689.7100 | 672.7310 | 1347.510 | 1461.750 |
| 1809 | 689.0101 | 668.4449 | 1345.850 | 1461.280 |
| 1810 | 688.3101 | 664.1590 | 1344.350 | 1461.240 |
| 1811 | 687.6100 | 659.8730 | 1342.850 | 1461.200 |
| 1812 | 686.9100 | 661.6440 | 1341.350 | 1461.160 |
| 1813 | 686.1512 | 669.4720 | 1339.850 | 1461.120 |
| 1814 | 684.8633 | 677.3000 | 1338.300 | 1460.510 |
| 1815 | 683.5753 | 685.1280 | 1336.700 | 1459.330 |
| 1816 | 682.2872 | 692.9560 | 1335.100 | 1458.150 |
| 1817 | 680.9993 | 695.3530 | 1333.500 | 1456.970 |
| 1818 | 679.7982 | 692.3190 | 1331.900 | 1455.790 |
| 1819 | 679.3802 | 689.2850 | 1330.280 | 1454.940 |
| 1820 | 678.9622 | 686.2510 | 1328.640 | 1454.420 |
| 1821 | 678.5443 | 683.2170 | 1327.000 | 1453.900 |
| 1822 | 678.1262 | 682.2050 | 1325.360 | 1453.380 |
| 1823 | 677.8986 | 683.2150 | 1323.720 | 1452.860 |
| 1824 | 679.3846 | 684.2250 | 1322.430 | 1452.790 |
| 1825 | 680.8705 | 685.2350 | 1321.490 | 1453.170 |
| 1826 | 682.3566 | 686.2450 | 1320.550 | 1453.550 |
| 1827 | 683.8425 | 689.3390 | 1319.610 | 1453.930 |
| 1828 | 685.4139 | 694.5170 | 1318.670 | 1454.310 |
| 1829 | 688.9499 | 699.6950 | 1318.320 | 1455.870 |
| 1830 | 693.3079 | 704.8730 | 1318.560 | 1458.610 |

Table 1 (*continued*)

| $E$ (eV) | Si-c | Si-a | $SiO_2$ | $Si_3N_4$ |
|---|---|---|---|---|
| 1831 | 700.8038 | 710.0510 | 1318.800 | 1461.350 |
| 1832 | 711.9236 | 719.9750 | 1319.040 | 1464.090 |
| 1833 | 728.7155 | 735.8950 | 1319.280 | 1466.830 |
| 1834 | 753.0652 | 758.7450 | 1320.000 | 1468.500 |
| 1835 | 794.5945 | 798.8700 | 1321.500 | 1493.000 |
| 1836 | 877.7345 | 875.6500 | 1323.700 | 1490.200 |
| 1837 | 1108.127 | 1087.385 | 1326.450 | 1502.500 |
| 1838 | 2390.250 | 2450.800 | 1330.000 | 1528.600 |
| 1839 | 7625.121 | 6987.200 | 1334.350 | 1592.400 |
| 1840 | 12684.77 | 11069.50 | 1340.850 | 1789.200 |
| 1841 | 13067.83 | 11538.00 | 1352.550 | 2305.300 |
| 1842 | 10917.64 | 10967.50 | 1371.850 | 3731.400 |
| 1843 | 10031.25 | 10522.00 | 1408.850 | 6806.000 |
| 1844 | 9808.678 | 10370.00 | 1494.900 | 10814.00 |
| 1845 | 10034.95 | 10380.50 | 1744.150 | 12219.00 |
| 1846 | 10574.58 | 10483.50 | 2606.800 | 11574.00 |
| 1847 | 10899.62 | 10454.00 | 5294.950 | 10704.00 |
| 1848 | 10180.19 | 10095.65 | 10480.40 | 10179.00 |
| 1849 | 9954.437 | 9702.650 | 11680.50 | 9228.200 |
| 1850 | 10119.40 | 9434.750 | 7634.450 | 8541.600 |
| 1851 | 10129.21 | 9234.050 | 5144.800 | 8276.500 |
| 1852 | 9693.937 | 9069.250 | 4685.550 | 8049.300 |
| 1853 | 9043.210 | 8941.200 | 4609.750 | 7861.300 |
| 1854 | 8685.827 | 8842.350 | 4560.450 | 7820.300 |
| 1855 | 8622.077 | 8759.301 | 4558.650 | 7848.300 |
| 1856 | 8553.958 | 8679.650 | 4594.100 | 7831.800 |
| 1857 | 8446.508 | 8603.600 | 4613.000 | 7862.800 |
| 1858 | 8338.862 | 8536.500 | 4595.950 | 7913.517 |
| 1859 | 8229.463 | 8479.801 | 4566.250 | 7986.950 |
| 1860 | 8125.961 | 8419.051 | 4565.350 | 8060.383 |
| 1861 | 8075.562 | 8347.400 | 4624.950 | 8052.450 |
| 1862 | 8038.968 | 8270.150 | 4740.200 | 7963.150 |
| 1863 | 8126.668 | 8179.500 | 4875.250 | 7873.850 |
| 1864 | 8205.920 | 8059.000 | 4987.600 | 7694.567 |
| 1865 | 8209.120 | 7910.100 | 5041.750 | 7425.300 |
| 1866 | 8195.249 | 7746.900 | 5021.050 | 7156.033 |
| 1867 | 8027.699 | 7580.000 | 4929.000 | 6918.050 |
| 1868 | 7850.811 | 7421.650 | 4780.050 | 6711.350 |
| 1869 | 7589.861 | 7280.850 | 4592.550 | 6504.650 |
| 1870 | 7330.496 | 7164.300 | 4383.600 | 6344.066 |
| 1871 | 7085.396 | 7072.200 | 4173.900 | 6229.600 |
| 1872 | 6857.137 | 7007.625 | 3985.150 | 6115.133 |
| 1873 | 6780.487 | 6959.075 | 3829.850 | 6027.533 |
| 1874 | 6715.389 | 6924.225 | 3716.667 | 5966.800 |
| 1875 | 6754.289 | 6903.075 | 3627.200 | 5906.067 |
| 1876 | 6793.544 | 6893.125 | 3537.733 | 5854.417 |
| 1877 | 6835.994 | 6894.375 | 3467.200 | 5811.850 |
| 1878 | 6877.354 | 6899.225 | 3415.600 | 5769.283 |
| 1879 | 6908.904 | 6907.675 | 3364.000 | 5734.617 |
| 1880 | 6947.552 | 6921.250 | 3325.983 | 5707.850 |
| 1881 | 7050.103 | 6939.950 | 3301.550 | 5681.083 |
| 1882 | 7145.214 | 6961.400 | 3277.117 | 5669.217 |
| 1883 | 7173.364 | 6985.600 | 3261.000 | 5672.250 |
| 1884 | 7192.812 | 7012.125 | 3253.200 | 5675.283 |
| 1885 | 7133.912 | 7040.975 | 3245.400 | 5682.400 |
| 1886 | 7072.092 | 7072.250 | 3241.100 | 5693.600 |
| 1887 | 6983.992 | 7105.950 | 3240.300 | 5704.800 |
| 1888 | 6898.152 | 7140.300 | 3239.500 | 5722.633 |

Table 1 (*continued*)

| $E$ (eV) | Si-c | Si-a | $SiO_2$ | $Si_3N_4$ |
|---|---|---|---|---|
| 1889 | 6832.652 | 7175.300 | 3241.450 | 5747.100 |
| 1890 | 6781.378 | 7211.225 | 3246.150 | 5771.566 |
| 1891 | 6858.178 | 7248.075 | 3250.850 | 5795.550 |
| 1892 | 6947.090 | 7282.150 | 3256.600 | 5819.050 |
| 1893 | 7145.040 | 7313.450 | 3263.400 | 5842.550 |
| 1894 | 7336.787 | 7339.950 | 3270.200 | 5871.816 |
| 1895 | 7472.687 | 7361.650 | 3276.667 | 5906.850 |
| 1896 | 7602.193 | 7375.775 | 3282.800 | 5941.883 |
| 1897 | 7674.143 | 7382.325 | 3288.933 | 5976.000 |
| 1898 | 7743.494 | 7380.775 | 3294.600 | 6009.200 |
| 1899 | 7789.444 | 7371.125 | 3299.800 | 6042.400 |
| 1900 | 7827.880 | 7352.150 | 3305.000 | 6073.783 |
| 1901 | 7798.681 | 7323.850 | 3310.733 | 6103.350 |
| 1902 | 7762.947 | 7288.900 | 3317.000 | 6132.917 |
| 1903 | 7668.397 | 7247.300 | 3323.267 | 6161.367 |
| 1904 | 7572.942 | 7201.175 | 3330.767 | 6188.700 |
| 1905 | 7469.342 | 7150.525 | 3339.500 | 6216.034 |
| 1906 | 7364.503 | 7098.600 | 3348.233 | 6238.083 |
| 1907 | 7248.503 | 7045.400 | 3358.817 | 6254.850 |
| 1908 | 7129.464 | 6990.925 | 3371.250 | 6271.617 |
| 1909 | 6983.063 | 6935.175 | 3383.683 | 6283.583 |
| 1910 | 6836.618 | 6882.400 | 3397.683 | 6290.750 |
| 1911 | 6689.769 | 6832.600 | 3413.250 | 6297.917 |
| 1912 | 6547.473 | 6783.825 | 3428.817 | 6298.417 |
| 1913 | 6446.172 | 6736.075 | 3445.433 | 6292.250 |
| 1914 | 6352.351 | 6691.775 | 3463.100 | 6286.083 |
| 1915 | 6325.851 | 6650.925 | 3480.767 | 6277.333 |
| 1916 | 6305.459 | 6613.175 | 3498.300 | 6266.000 |
| 1917 | 6340.059 | 6578.525 | 3515.700 | 6254.667 |
| 1918 | 6373.930 | 6545.350 | 3533.100 | 6240.800 |
| 1919 | 6401.229 | 6513.650 | 3548.867 | 6224.400 |
| 1920 | 6425.025 | 6488.975 | 3563.000 | 6208.000 |
| 1921 | 6417.275 | 6471.325 | 3577.133 | 6203.883 |
| 1922 | 6408.900 | 6451.725 | 3588.367 | 6212.050 |
| 1923 | 6394.900 | 6430.175 | 3596.700 | 6220.216 |
| 1924 | 6382.455 | 6411.750 | 3605.033 | 6205.417 |
| 1925 | 6384.005 | 6396.450 | 3609.883 | 6167.650 |
| 1926 | 6387.669 | 6383.750 | 3611.250 | 6129.883 |
| 1927 | 6410.369 | 6373.650 | 3612.617 | 6103.184 |
| 1928 | 6434.224 | 6365.175 | 3611.067 | 6087.550 |
| 1929 | 6468.474 | 6358.325 | 3606.600 | 6071.917 |
| 1930 | 6501.034 | 6353.875 | 3602.133 | 6057.783 |
| 1931 | 6518.384 | 6351.825 | 3596.333 | 6045.150 |
| 1932 | 6533.400 | 6351.550 | 3589.200 | 6032.517 |
| 1933 | 6527.400 | 6353.050 | 3582.067 | 6023.383 |
| 1934 | 6519.951 | 6357.125 | 3574.983 | 6017.750 |
| 1935 | 6499.451 | 6363.775 | 3567.950 | 6012.117 |
| 1936 | 6479.226 | 6371.975 | 3560.917 | 6007.850 |
| 1937 | 6461.476 | 6381.725 | 3554.283 | 6004.950 |
| 1938 | 6444.615 | 6392.825 | 3548.050 | 6002.050 |
| 1939 | 6435.765 | 6405.275 | 3541.817 | 5995.550 |
| 1940 | 6427.295 | 6418.400 | 3535.467 | 5985.450 |
| 1941 | 6422.245 | 6432.200 | 3529.000 | 5975.350 |
| 1942 | 6417.510 | 6445.700 | 3522.533 | 5964.183 |
| 1943 | 6415.610 | 6458.900 | 3515.433 | 5951.950 |
| 1944 | 6413.545 | 6472.800 | 3507.700 | 5939.717 |
| 1945 | 6409.995 | 6487.400 | 3499.967 | 5927.767 |
| 1946 | 6405.800 | 6499.375 | 3491.483 | 5916.100 |

Table 1 (*continued*)

| $E$ (eV) | Si-c | Si-a | $SiO_2$ | $Si_3N_4$ |
|---|---|---|---|---|
| 1947 | 6395.800 | 6508.725 | 3482.250 | 5904.434 |
| 1948 | 6385.975 | 6517.650 | 3473.017 | 5890.750 |
| 1949 | 6377.725 | 6526.150 | 3463.150 | 5875.050 |
| 1950 | 6371.109 | 6532.800 | 3452.650 | 5859.350 |
| 1951 | 6379.209 | 6537.600 | 3442.150 | 5845.767 |
| 1952 | 6388.569 | 6540.950 | 3431.317 | 5834.300 |
| 1953 | 6409.270 | 6542.850 | 3420.150 | 5822.833 |
| 1954 | 6429.620 | 6542.650 | 3408.983 | 5810.025 |
| 1955 | 6446.819 | 6540.350 | 3397.517 | 5795.875 |
| 1956 | 6463.939 | 6535.800 | 3385.750 | 5781.725 |
| 1957 | 6480.339 | 6529.000 | 3373.983 | 5767.575 |
| 1958 | 6496.975 | 6520.625 | 3362.250 | 5753.425 |
| 1959 | 6515.725 | 6510.675 | 3350.550 | 5739.275 |
| 1960 | 6534.944 | 6500.000 | 3338.850 | 5725.125 |
| 1961 | 6558.395 | 6488.600 | 3327.300 | 5710.975 |
| 1962 | 6581.895 | 6475.125 | 3315.900 | 5699.181 |
| 1963 | 6605.844 | 6459.575 | 3304.500 | 5689.744 |
| 1964 | 6628.250 | 6443.800 | 3293.600 | 5680.306 |
| 1965 | 6636.750 | 6427.800 | 3283.200 | 5670.869 |
| 1966 | 6642.396 | 6412.650 | 3272.800 | 5661.431 |
| 1967 | 6622.345 | 6398.350 | 3262.400 | 5651.994 |
| 1968 | 6599.886 | 6383.500 | 3252.000 | 5642.556 |
| 1969 | 6555.736 | 6368.100 | 3241.600 | 5633.119 |
| 1970 | 6511.146 | 6350.050 | 3232.475 | 5628.325 |
| 1971 | 6462.596 | 6329.350 | 3224.625 | 5628.175 |
| 1972 | 6414.876 | 6309.375 | 3216.775 | 5628.025 |
| 1973 | 6374.626 | 6290.125 | 3208.925 | 5627.875 |
| 1974 | 6335.601 | 6276.825 | 3201.075 | 5627.725 |
| 1975 | 6307.601 | 6269.475 | 3193.225 | 5627.575 |
| 1976 | 6279.985 | 6258.100 | 3187.583 | 5627.425 |
| 1977 | 6255.835 | 6242.700 | 3184.150 | 5627.275 |
| 1978 | 6230.726 | 6226.675 | 3180.717 | 5628.775 |
| 1979 | 6196.976 | 6210.025 | 3177.283 | 5631.925 |
| 1980 | 6162.766 | 6192.775 | 3173.850 | 5635.075 |
| 1981 | 6124.416 | 6174.925 | 3170.417 | 5638.225 |
| 1982 | 6086.301 | 6158.225 | 3167.417 | 5641.375 |
| 1983 | 6050.301 | 6142.675 | 3164.850 | 5644.525 |
| 1984 | 6016.350 | 6127.425 | 3162.283 | 5647.675 |
| 1985 | 6000.850 | 6112.475 | 3159.717 | 5650.825 |
| 1986 | 5987.030 | 6098.075 | 3157.150 | 5653.987 |
| 1987 | 5988.330 | 6084.225 | 3154.583 | 5657.163 |
| 1988 | 5989.325 | 6070.850 | 3151.975 | 5660.337 |
| 1989 | 5987.575 | 6057.950 | 3149.325 | 5663.512 |
| 1990 | 5985.400 | 6045.225 | 3146.675 | 5666.688 |
| 1991 | 5979.400 | 6032.675 | 3144.025 | 5669.862 |
| 1992 | 5973.520 | 6021.400 | 3141.375 | 5673.037 |
| 1993 | 5968.720 | 6011.400 | 3138.725 | 5676.212 |
| 1994 | 5963.700 | 6002.675 | 3137.542 | 5678.650 |
| 1995 | 5956.700 | 5995.225 | 3137.825 | 5680.350 |
| 1996 | 5949.620 | 5988.000 | 3138.108 | 5682.050 |
| 1997 | 5941.820 | 5981.000 | 3138.392 | 5683.750 |
| 1998 | 5934.280 | 5975.150 | 3138.675 | 5685.450 |
| 1999 | 5929.080 | 5970.450 | 3138.958 | 5687.150 |
| 2000 | 5923.880 | 5966.375 | 3139.042 | 5688.850 |
| 2001 | 5918.680 | 5962.925 | 3138.925 | 5690.550 |
| 2002 | 5913.480 | 5960.075 | 3138.808 | 5691.900 |
| 2003 | 5908.952 | 5957.825 | 3138.692 | 5692.900 |
| 2004 | 5910.472 | 5956.100 | 3138.575 | 5693.900 |

Table 1 (*continued*)

| $E$ (eV) | Si-c | Si-a | $SiO_2$ | $Si_3N_4$ |
|---|---|---|---|---|
| 2005 | 5911.992 | 5954.900 | 3138.458 | 5694.900 |
| 2006 | 5913.512 | 5954.350 | 3138.600 | 5695.900 |
| 2007 | 5915.032 | 5954.450 | 3139.000 | 5696.900 |
| 2008 | 5917.352 | 5955.075 | 3139.400 | 5697.900 |
| 2009 | 5926.872 | 5956.225 | 3139.800 | 5698.900 |
| 2010 | 5936.392 | 5957.325 | 3140.200 | 5697.431 |
| 2011 | 5945.912 | 5958.375 | 3140.600 | 5693.494 |
| 2012 | 5955.432 | 5960.850 | 3141.517 | 5689.556 |
| 2013 | 5964.242 | 5964.750 | 3142.950 | 5685.619 |
| 2014 | 5966.662 | 5968.050 | 3144.383 | 5681.681 |
| 2015 | 5969.082 | 5970.750 | 3145.817 | 5677.744 |
| 2016 | 5971.502 | 5973.700 | 3147.250 | 5673.806 |
| 2017 | 5973.922 | 5976.900 | 3148.683 | 5669.869 |
| 2018 | 5976.188 | 5978.775 | 3149.983 | 5666.369 |
| 2019 | 5977.068 | 5979.325 | 3151.150 | 5663.306 |
| 2020 | 5977.948 | 5980.925 | 3152.317 | 5660.244 |
| 2021 | 5978.828 | 5983.575 | 3153.483 | 5657.181 |
| 2022 | 5979.708 | 5985.600 | 3154.650 | 5654.119 |
| 2023 | 5980.456 | 5987.000 | 3155.817 | 5651.056 |
| 2024 | 5980.016 | 5987.575 | 3156.950 | 5647.994 |
| 2025 | 5979.576 | 5987.325 | 3158.050 | 5644.931 |
| 2026 | 5979.136 | 5987.775 | 3159.150 | 5638.793 |
| 2027 | 5978.696 | 5988.925 | 3160.250 | 5629.581 |
| 2028 | 5976.670 | 5986.650 | 3161.350 | 5620.369 |
| 2029 | 5960.370 | 5980.950 | 3162.450 | 5611.156 |
| 2030 | 5944.070 | 5975.775 | 3161.642 | 5601.944 |
| 2031 | 5927.770 | 5971.125 | 3158.925 | 5592.731 |
| 2032 | 5911.470 | 5967.000 | 3156.208 | 5583.519 |
| 2033 | 5897.380 | 5963.400 | 3153.492 | 5574.307 |
| 2034 | 5903.180 | 5957.225 | 3150.775 | 5566.531 |
| 2035 | 5908.979 | 5948.475 | 3148.058 | 5560.194 |
| 2036 | 5914.780 | 5939.725 | 3145.167 | 5553.856 |
| 2037 | 5920.580 | 5930.975 | 3142.100 | 5547.519 |
| 2038 | 5925.242 | 5923.525 | 3139.033 | 5541.181 |
| 2039 | 5919.662 | 5917.375 | 3135.967 | 5534.844 |
| 2040 | 5914.082 | 5909.575 | 3132.900 | 5528.506 |
| 2041 | 5908.502 | 5900.125 | 3129.833 | 5522.169 |
| 2042 | 5902.922 | 5890.475 | 3126.817 | 5515.294 |
| 2043 | 5896.094 | 5880.625 | 3123.850 | 5507.881 |
| 2044 | 5878.034 | 5870.600 | 3120.883 | 5500.469 |
| 2045 | 5859.975 | 5860.400 | 3117.917 | 5493.056 |
| 2046 | 5841.915 | 5849.975 | 3114.950 | 5485.644 |
| 2047 | 5823.854 | 5839.325 | 3111.983 | 5478.231 |
| 2048 | 5806.077 | 5828.550 | 3109.067 | 5470.819 |
| 2049 | 5790.836 | 5817.650 | 3106.200 | 5463.406 |
| 2050 | 5775.596 | 5806.475 | 3103.333 | 5456.981 |
| 2051 | 5760.355 | 5795.025 | 3100.467 | 5451.544 |
| 2052 | 5745.115 | 5784.025 | 3097.600 | 5446.106 |
| 2053 | 5730.861 | 5773.475 | 3094.733 | 5440.669 |
| 2054 | 5725.481 | 5762.250 | 3091.958 | 5435.231 |
| 2055 | 5720.102 | 5750.350 | 3089.275 | 5429.794 |
| 2056 | 5714.722 | 5738.675 | 3086.592 | 5424.356 |
| 2057 | 5709.341 | 5727.225 | 3083.908 | 5418.919 |
| 2058 | 5704.360 | 5717.000 | 3081.225 | 5413.394 |
| 2059 | 5702.960 | 5708.000 | 3078.542 | 5407.781 |
| 2060 | 5701.560 | 5698.425 | 3075.833 | 5402.169 |
| 2061 | 5700.160 | 5688.275 | 3073.100 | 5396.556 |
| 2062 | 5698.760 | 5680.000 | 3070.367 | 5390.944 |

Table 1 (*continued*)

| $E$ (eV) | Si-c | Si-a | $SiO_2$ | $Si_3N_4$ |
|---|---|---|---|---|
| 2063 | 5696.303 | 5673.600 | 3067.633 | 5385.331 |
| 2064 | 5684.343 | 5662.975 | 3064.900 | 5379.719 |
| 2065 | 5672.383 | 5648.125 | 3062.167 | 5374.106 |
| 2066 | 5660.423 | 5637.075 | 3059.208 | 5367.981 |
| 2067 | 5648.463 | 5629.825 | 3056.025 | 5361.344 |
| 2068 | 5636.623 | 5621.575 | 3052.842 | 5354.706 |
| 2069 | 5625.863 | 5612.325 | 3049.658 | 5348.069 |
| 2070 | 5615.103 | 5603.475 | 3046.475 | 5341.431 |
| 2071 | 5604.343 | 5595.025 | 3043.292 | 5334.794 |
| 2072 | 5593.583 | 5586.850 | 3039.925 | 5328.156 |
| 2073 | 5582.791 | 5578.950 | 3036.375 | 5321.519 |
| 2074 | 5571.711 | 5571.200 | 3032.825 | 5315.013 |
| 2075 | 5560.631 | 5563.600 | 3029.275 | 5308.638 |
| 2076 | 5549.551 | 5556.575 | 3025.725 | 5302.263 |
| 2077 | 5538.471 | 5550.125 | 3022.175 | 5295.888 |
| 2078 | 5527.511 | 5543.625 | 3018.350 | 5289.513 |
| 2079 | 5517.631 | 5537.075 | 3014.250 | 5283.138 |
| 2080 | 5507.751 | 5530.700 | 3010.150 | 5276.763 |
| 2081 | 5497.871 | 5524.500 | 3006.050 | 5270.388 |
| 2082 | 5487.991 | 5518.250 | 3001.950 | 5264.557 |
| 2083 | 5478.624 | 5511.950 | 2997.850 | 5259.269 |
| 2084 | 5473.864 | 5507.275 | 2993.575 | 5253.981 |
| 2085 | 5469.104 | 5504.225 | 2989.125 | 5248.694 |
| 2086 | 5464.343 | 5498.800 | 2984.675 | 5243.406 |
| 2087 | 5459.583 | 5491.000 | 2980.225 | 5238.119 |
| 2088 | 5454.917 | 5485.350 | 2975.775 | 5232.831 |
| 2089 | 5451.098 | 5481.850 | 2971.325 | 5227.543 |
| 2090 | 5447.278 | 5478.525 | 2967.400 | 5222.387 |
| 2091 | 5443.458 | 5475.375 | 2964.000 | 5217.362 |
| 2092 | 5439.638 | 5471.275 | 2960.600 | 5212.337 |
| 2093 | 5435.729 | 5466.225 | 2957.200 | 5207.313 |
| 2094 | 5431.030 | 5463.625 | 2953.800 | 5202.288 |
| 2095 | 5426.330 | 5463.475 | 2950.400 | 5197.263 |
| 2096 | 5421.630 | 5461.075 | 2946.267 | 5192.238 |
| 2097 | 5416.930 | 5456.425 | 2941.400 | 5187.213 |
| 2098 | 5412.118 | 5452.075 | 2936.533 | 5182.707 |
| 2099 | 5406.297 | 5448.025 | 2931.667 | 5178.719 |
| 2100 | 5400.478 | 5444.450 | 2926.800 | 5174.731 |
| 2101 | 5394.658 | 5441.350 | 2921.933 | 5170.744 |
| 2102 | 5388.837 | 5438.220 | 2917.600 | 5166.756 |
| 2103 | 5383.728 | 5435.060 | 2913.800 | 5162.769 |
| 2104 | 5385.008 | 5431.900 | 2910.000 | 5158.781 |
| 2105 | 5386.288 | 5428.740 | 2906.200 | 5154.793 |
| 2106 | 5387.568 | 5425.580 | 2902.400 | 5152.025 |
| 2107 | 5388.848 | 5422.330 | 2898.600 | 5150.475 |
| 2108 | 5390.012 | 5418.990 | 2895.050 | 5148.925 |
| 2109 | 5390.132 | 5415.650 | 2891.750 | 5147.375 |
| 2110 | 5390.252 | 5412.310 | 2888.450 | 5145.825 |
| 2111 | 5390.372 | 5408.970 | 2885.150 | 5144.275 |
| 2112 | 5390.492 | 5405.420 | 2881.850 | 5142.725 |
| 2113 | 5390.472 | 5401.660 | 2878.550 | 5141.175 |
| 2114 | 5389.192 | 5397.900 | 2875.492 | 5139.350 |
| 2115 | 5387.912 | 5394.140 | 2872.675 | 5137.250 |
| 2116 | 5386.632 | 5390.380 | 2869.858 | 5135.150 |
| 2117 | 5385.352 | 5386.370 | 2867.042 | 5133.050 |
| 2118 | 5384.060 | 5382.110 | 2864.225 | 5130.950 |
| 2119 | 5382.660 | 5377.850 | 2861.408 | 5128.850 |
| 2120 | 5381.260 | 5373.590 | 2858.825 | 5126.750 |

Table 1 (*continued*)

| $E$ (eV) | Si-c | Si-a | $SiO_2$ | $Si_3N_4$ |
|---|---|---|---|---|
| 2121 | 5379.860 | 5369.330 | 2856.475 | 5124.650 |
| 2122 | 5378.460 | 5364.820 | 2854.125 | 5121.431 |
| 2123 | 5376.992 | 5360.060 | 2851.775 | 5117.094 |
| 2124 | 5374.912 | 5355.300 | 2849.425 | 5112.756 |
| 2125 | 5372.832 | 5350.540 | 2847.075 | 5108.419 |
| 2126 | 5370.752 | 5345.780 | 2844.958 | 5104.081 |
| 2127 | 5368.672 | 5340.630 | 2843.075 | 5099.744 |
| 2128 | 5366.053 | 5335.090 | 2841.192 | 5095.406 |
| 2129 | 5358.593 | 5329.550 | 2839.308 | 5091.069 |
| 2130 | 5351.133 | 5324.010 | 2837.425 | 5087.581 |
| 2131 | 5343.673 | 5318.470 | 2835.542 | 5084.944 |
| 2132 | 5336.213 | 5312.700 | 2833.825 | 5082.306 |
| 2133 | 5328.191 | 5306.700 | 2832.275 | 5079.668 |
| 2134 | 5315.111 | 5300.700 | 2830.725 | 5077.031 |
| 2135 | 5302.031 | 5294.700 | 2829.175 | 5074.394 |
| 2136 | 5288.951 | 5288.700 | 2827.625 | 5071.756 |
| 2137 | 5275.871 | 5282.510 | 2826.075 | 5069.119 |
| 2138 | 5263.081 | 5276.130 | 2824.650 | 5066.156 |
| 2139 | 5252.901 | 5269.750 | 2823.350 | 5062.869 |
| 2140 | 5242.721 | 5263.370 | 2822.050 | 5059.581 |
| 2141 | 5232.541 | 5256.990 | 2820.750 | 5056.293 |
| 2142 | 5222.361 | 5250.260 | 2819.450 | 5053.006 |
| 2143 | 5212.463 | 5243.180 | 2818.150 | 5049.719 |
| 2144 | 5205.104 | 5236.100 | 2816.500 | 5046.431 |
| 2145 | 5197.743 | 5229.020 | 2814.500 | 5043.144 |
| 2146 | 5190.383 | 5221.940 | 2812.500 | 5038.556 |
| 2147 | 5183.023 | 5214.070 | 2810.500 | 5032.669 |
| 2148 | 5175.681 | 5205.410 | 2808.500 | 5026.781 |
| 2149 | 5168.501 | 5196.750 | 2806.500 | 5020.894 |
| 2150 | 5161.321 | 5188.090 | 2805.167 | 5015.006 |
| 2151 | 5154.141 | 5179.430 | 2804.500 | 5009.119 |
| 2152 | 5146.961 | 5172.600 | 2803.833 | 5003.231 |
| 2153 | 5140.056 | 5167.600 | 2803.167 | 4997.344 |
| 2154 | 5135.616 | 5162.600 | 2802.500 | 4991.487 |
| 2155 | 5131.175 | 5157.600 | 2801.833 | 4985.663 |
| 2156 | 5126.735 | 5152.600 | 2800.883 | 4979.837 |
| 2157 | 5122.295 | 5146.950 | 2799.650 | 4974.012 |
| 2158 | 5117.711 | 5140.650 | 2798.417 | 4968.188 |
| 2159 | 5111.831 | 5134.350 | 2797.183 | 4962.362 |
| 2160 | 5105.951 | 5128.050 | 2795.950 | 4956.537 |
| 2161 | 5100.071 | 5121.750 | 2794.717 | 4950.712 |
| 2162 | 5094.191 | 5115.550 | 2793.342 | 4945.225 |
| 2163 | 5088.350 | 5109.450 | 2791.825 | 4940.075 |
| 2164 | 5082.850 | 5103.350 | 2790.308 | 4934.925 |
| 2165 | 5077.350 | 5097.250 | 2788.792 | 4929.775 |
| 2166 | 5071.850 | 5091.150 | 2787.275 | 4924.625 |
| 2167 | 5066.350 | 5085.450 | 2785.758 | 4919.475 |
| 2168 | 5061.092 | 5080.150 | 2784.300 | 4914.325 |
| 2169 | 5058.012 | 5074.850 | 2782.900 | 4909.175 |
| 2170 | 5054.932 | 5069.550 | 2781.500 | 4904.332 |
| 2171 | 5051.852 | 5064.250 | 2780.100 | 4899.794 |
| 2172 | 5048.771 | 5059.180 | 2778.700 | 4895.256 |
| 2173 | 5045.583 | 5054.340 | 2777.300 | 4890.719 |
| 2174 | 5041.424 | 5049.500 | 2775.767 | 4886.181 |
| 2175 | 5037.264 | 5044.660 | 2774.100 | 4881.644 |
| 2176 | 5033.104 | 5039.820 | 2772.433 | 4877.106 |
| 2177 | 5028.944 | 5035.070 | 2770.767 | 4872.568 |
| 2178 | 5024.722 | 5030.410 | 2769.100 | 4867.900 |

Table 1 (*continued*)

| $E$ (eV) | Si-c | Si-a | $SiO_2$ | $Si_3N_4$ |
|---|---|---|---|---|
| 2179 | 5019.941 | 5025.750 | 2767.433 | 4863.100 |
| 2180 | 5015.162 | 5021.090 | 2765.633 | 4858.300 |
| 2181 | 5010.381 | 5016.430 | 2763.700 | 4853.500 |
| 2182 | 5005.602 | 5011.900 | 2761.767 | 4848.700 |
| 2183 | 5000.905 | 5007.500 | 2759.833 | 4843.900 |
| 2184 | 4996.965 | 5003.100 | 2757.900 | 4839.100 |
| 2185 | 4993.025 | 4998.700 | 2755.967 | 4834.300 |
| 2186 | 4989.085 | 4994.300 | 2753.933 | 4829.381 |
| 2187 | 4985.146 | 4990.020 | 2751.800 | 4824.344 |
| 2188 | 4981.134 | 4985.860 | 2749.667 | 4819.306 |
| 2189 | 4976.474 | 4981.700 | 2747.533 | 4814.269 |
| 2190 | 4971.813 | 4977.540 | 2745.400 | 4809.231 |
| 2191 | 4967.153 | 4973.380 | 2743.267 | 4804.194 |
| 2192 | 4962.493 | 4969.650 | 2741.542 | 4799.156 |
| 2193 | 4957.881 | 4966.350 | 2740.225 | 4794.119 |
| 2194 | 4953.702 | 4963.050 | 2738.908 | 4789.625 |
| 2195 | 4949.521 | 4959.750 | 2737.592 | 4785.675 |
| 2196 | 4945.341 | 4956.450 | 2736.275 | 4781.725 |
| 2197 | 4941.162 | 4952.760 | 2734.958 | 4777.775 |
| 2198 | 4936.989 | 4948.680 | 2733.025 | 4773.825 |
| 2199 | 4932.890 | 4944.600 | 2730.475 | 4769.875 |
| 2200 | 4928.790 | 4940.520 | 2727.925 | 4765.925 |
| 2201 | 4924.689 | 4936.440 | 2725.375 | 4761.975 |
| 2202 | 4920.589 | 4932.590 | 2722.825 | 4758.362 |
| 2203 | 4916.459 | 4928.970 | 2720.275 | 4755.087 |
| 2204 | 4912.060 | 4925.350 | 2717.942 | 4751.813 |
| 2205 | 4907.660 | 4921.730 | 2715.825 | 4748.538 |
| 2206 | 4903.259 | 4918.110 | 2713.708 | 4745.262 |
| 2207 | 4898.859 | 4914.540 | 2711.592 | 4741.987 |
| 2208 | 4894.543 | 4911.020 | 2709.475 | 4738.712 |
| 2209 | 4890.983 | 4907.500 | 2707.358 | 4735.438 |
| 2210 | 4887.424 | 4903.980 | 2705.275 | 4732.031 |
| 2211 | 4883.864 | 4900.460 | 2703.225 | 4728.494 |
| 2212 | 4880.304 | 4896.850 | 2701.175 | 4724.956 |
| 2213 | 4876.804 | 4893.150 | 2699.125 | 4721.418 |
| 2214 | 4873.844 | 4889.450 | 2697.075 | 4717.881 |
| 2215 | 4870.884 | 4885.750 | 2695.025 | 4714.344 |
| 2216 | 4867.924 | 4882.050 | 2692.925 | 4710.806 |
| 2217 | 4864.963 | 4878.250 | 2690.775 | 4707.269 |
| 2218 | 4862.072 | 4874.350 | 2688.625 | 4702.844 |
| 2219 | 4859.792 | 4870.450 | 2686.475 | 4697.531 |
| 2220 | 4857.512 | 4866.550 | 2684.325 | 4692.219 |
| 2221 | 4855.231 | 4862.650 | 2682.175 | 4686.906 |
| 2222 | 4852.952 | 4858.750 | 2680.033 | 4681.594 |
| 2223 | 4850.712 | 4854.850 | 2677.900 | 4676.281 |
| 2224 | 4848.832 | 4850.950 | 2675.767 | 4670.969 |
| 2225 | 4846.952 | 4847.050 | 2673.633 | 4665.656 |
| 2226 | 4845.072 | 4843.150 | 2671.500 | 4661.481 |
| 2227 | 4843.192 | 4839.140 | 2669.367 | 4658.444 |
| 2228 | 4841.212 | 4835.020 | 2667.200 | 4655.406 |
| 2229 | 4838.332 | 4830.900 | 2665.000 | 4652.369 |
| 2230 | 4835.452 | 4826.780 | 2662.800 | 4649.332 |
| 2231 | 4832.572 | 4822.660 | 2660.600 | 4646.294 |
| 2232 | 4829.692 | 4818.510 | 2658.400 | 4643.256 |
| 2233 | 4826.658 | 4814.330 | 2656.200 | 4640.219 |
| 2234 | 4822.238 | 4810.150 | 2654.000 | 4636.381 |
| 2235 | 4817.817 | 4805.970 | 2651.800 | 4631.744 |
| 2236 | 4813.397 | 4801.790 | 2649.600 | 4627.106 |

Table 1 (*continued*)

| $E$ (eV) | Si-c | Si-a | $SiO_2$ | $Si_3N_4$ |
|---|---|---|---|---|
| 2237 | 4808.978 | 4797.470 | 2647.400 | 4622.469 |
| 2238 | 4804.656 | 4793.010 | 2645.200 | 4617.832 |
| 2239 | 4801.216 | 4788.550 | 2643.000 | 4613.194 |
| 2240 | 4797.775 | 4784.090 | 2640.758 | 4608.556 |
| 2241 | 4794.335 | 4779.630 | 2638.475 | 4603.919 |
| 2242 | 4790.896 | 4775.120 | 2636.192 | 4599.938 |
| 2243 | 4787.452 | 4770.560 | 2633.908 | 4596.613 |
| 2244 | 4783.972 | 4766.000 | 2631.625 | 4593.288 |
| 2245 | 4780.492 | 4761.440 | 2629.342 | 4589.962 |
| 2246 | 4777.012 | 4756.880 | 2627.017 | 4586.638 |
| 2247 | 4773.532 | 4752.290 | 2624.650 | 4583.313 |
| 2248 | 4769.905 | 4747.670 | 2622.283 | 4579.987 |
| 2249 | 4764.965 | 4743.050 | 2619.917 | 4576.663 |
| 2250 | 4760.025 | 4738.430 | 2617.550 | 4573.737 |
| 2251 | 4755.085 | 4733.810 | 2615.183 | 4571.212 |
| 2252 | 4750.146 | 4729.140 | 2612.858 | 4568.688 |
| 2253 | 4745.029 | 4724.420 | 2610.575 | 4566.163 |
| 2254 | 4738.330 | 4719.700 | 2608.292 | 4563.637 |
| 2255 | 4731.629 | 4714.980 | 2606.008 | 4561.112 |
| 2256 | 4724.930 | 4710.260 | 2603.725 | 4558.587 |
| 2257 | 4718.229 | 4705.540 | 2601.442 | 4556.063 |
| 2258 | 4711.572 | 4700.820 | 2599.167 | 4553.400 |
| 2259 | 4705.292 | 4696.100 | 2596.900 | 4550.600 |
| 2260 | 4699.011 | 4691.380 | 2594.633 | 4547.800 |
| 2261 | 4692.731 | 4686.660 | 2592.367 | 4545.000 |
| 2262 | 4686.451 | 4681.940 | 2590.100 | 4542.200 |
| 2263 | 4680.285 | 4677.220 | 2587.833 | 4539.400 |
| 2264 | 4675.146 | 4672.500 | 2585.650 | 4536.600 |
| 2265 | 4670.005 | 4667.780 | 2583.550 | 4533.800 |
| 2266 | 4664.866 | 4663.060 | 2581.450 | 4531.087 |
| 2267 | 4659.726 | 4658.430 | 2579.350 | 4528.462 |
| 2268 | 4654.520 | 4653.890 | 2577.250 | 4525.837 |
| 2269 | 4648.720 | 4649.350 | 2575.150 | 4523.212 |
| 2270 | 4642.919 | 4644.810 | 2573.083 | 4520.587 |
| 2271 | 4637.120 | 4640.270 | 2571.050 | 4517.962 |
| 2272 | 4631.319 | 4635.780 | 2569.017 | 4515.337 |
| 2273 | 4625.642 | 4631.340 | 2566.983 | 4512.712 |
| 2274 | 4621.062 | 4626.900 | 2564.950 | 4509.788 |
| 2275 | 4616.482 | 4622.460 | 2562.917 | 4506.563 |
| 2276 | 4611.902 | 4618.020 | 2560.967 | 4503.337 |
| 2277 | 4607.322 | 4613.660 | 2559.100 | 4500.112 |
| 2278 | 4602.760 | 4609.380 | 2557.233 | 4496.888 |
| 2279 | 4598.360 | 4605.100 | 2555.367 | 4493.663 |
| 2280 | 4593.960 | 4600.820 | 2553.500 | 4490.438 |
| 2281 | 4589.560 | 4596.540 | 2551.633 | 4487.212 |
| 2282 | 4585.160 | 4592.300 | 2549.808 | 4483.300 |
| 2283 | 4580.776 | 4588.100 | 2548.025 | 4478.700 |
| 2284 | 4576.536 | 4583.900 | 2546.242 | 4474.100 |
| 2285 | 4572.296 | 4579.700 | 2544.458 | 4469.500 |
| 2286 | 4568.056 | 4575.500 | 2542.675 | 4464.900 |
| 2287 | 4563.815 | 4571.430 | 2540.892 | 4460.300 |
| 2288 | 4559.640 | 4567.490 | 2539.192 | 4455.700 |
| 2289 | 4556.040 | 4563.550 | 2537.575 | 4451.100 |
| 2290 | 4552.439 | 4559.610 | 2535.958 | 4447.750 |
| 2291 | 4548.840 | 4555.670 | 2534.342 | 4445.650 |
| 2292 | 4545.240 | 4551.840 | 2532.725 | 4443.550 |
| 2293 | 4541.729 | 4548.120 | 2531.108 | 4441.450 |
| 2294 | 4539.030 | 4544.400 | 2529.517 | 4439.350 |

Table 1 (*continued*)

| $E$ (eV) | Si-c | Si-a | $SiO_2$ | $Si_3N_4$ |
|---|---|---|---|---|
| 2295 | 4536.330 | 4540.680 | 2527.950 | 4437.250 |
| 2296 | 4533.630 | 4536.960 | 2526.383 | 4435.150 |
| 2297 | 4530.930 | 4533.220 | 2524.817 | 4433.050 |
| 2298 | 4528.189 | 4529.460 | 2523.250 | 4430.888 |
| 2299 | 4525.090 | 4525.700 | 2521.683 | 4428.663 |
| 2300 | 4521.990 | 4521.940 | 2520.167 | 4426.438 |

Please note that the number of significant places after the decimal points is an artefact of the computer program used to produce them and is not intended to imply statistical precision. The typical uncertainty on the measured data points is estimated to be at the few percent level and on the interpolated values given in the table, about a factor of two lower. The coefficients may be converted into mass attenuation coefficients, $\mu/\rho$, by dividing by the appropriate density, i.e., $\rho(Si) \equiv 2.329\,g/cm^3$ (crystalline; Tatsumi and Ohsaki, 1988) and $2.1\,g/cm^3$ (amorphous—averaged vacuum evaporation and sputtered; Tatsumi and Ohsaki, 1988), $\rho(SiO_2) \equiv 2.200\,g/cm^3$ (film and bulk; Peterson, 1978) and $2.27\,g/cm^3$ (thermal dry oxide; El-Kareh, 1995) and $\rho(Si_3N_4) \equiv 3.2\,g/cm^3$ (ceramic; Ohji et al., 1990) and $3.100\,g/cm^3$ (sputtered; Peterson, 1978). Note, the densities quoted are representative of quoted values, however, it should be noted that the densities of commercial material can vary by a few percent depending on the exact production process used.

Debye–Waller factors of $\sim 0.01$ and 0.04 for the crystalline and amorphous materials, respectively. These can be considered representative for MOS construction. For completeness, we have derived linear attenuation coefficients from 1800 to 2300 eV in 1 eV steps by interpolation of the experimental data. The results are tabulated in Table 1. It should be noted that because of the narrow width of the dioxide white line, the data are undersampled. In fact, we estimate by fitting the line using data with 0.5 eV spacing, that the peak is 10% larger. The error in the energy determination is not more than 1 eV and typical uncertainties in the listed coefficients are estimated to be at the few percent level.

### 3.1. Calculating linear attenuation coefficients

Lastly, we point out that there is an approximate method for calculating linear attenuation coefficients if experimental data is not available—for example, near the oxygen and nitrogen edges where suitable synchrotron beamlines are limited. From Fig. 3, we note that the calculations of Cromer and Liberman (1970) accurately reproduce the trend in $\mu(E)$, but show no structure. This is expected, since the theory is only applicable for isolated atoms and does not include modifications to the wavefunction by neighboring atoms. Also, because the calculations of Cromer and Liberman are so computationally intensive, they were only calculated at a few energy points and intermediate values interpolated by a smooth function of energy. This in turn tends to wash out the peak at the absorption edge—the 'white line'. Gurman (1983) has reported an approximate theory for calculating $\mu(E)$ accurately and rapidly for the isolated atom. This rapidity allows many more energy points to be calculated and in this way the 'white line' may be found. The oscillatory structure which extends several hundred eV or more above the edge (the extended X-ray absorption fine structure (EXAFS)) can then be calculated by standard methods (e.g., spherical wave approximation; Gurman, 1990) and added. In this way, $\mu(E)$ can be accurately 'built-up'. Obviously, X-ray absorption near-edge structure (XANES) due to multiple scattering effects (Bianconi et al., 1987) will not be present, which will result in a loss of detail within $\sim 70$ eV of the edge.

## Acknowledgements

This work was supported by the Daresbury Laboratory SESS and the SERC. We thank A.D. Smith for beamline support and S. Bayliss for providing the $Si_3N_4$ data.

## References

Bianconi, A., di Cicco, A., Pavel, N.V., Benfatto, M., Marcelli, A., Natoli, C.R., Pianetta, P., Woicik, J., 1987. Multiple-scattering effects in the K-edge X-ray-absorption near-edge structure of crystalline and amorphous silicon. Phys. Rev. B 36, 6426–6433.

Cho, T., Yamaguchi, N., Kondoh, T., Hirata, M., Miyoshi, S., Aoki, S., Maezawa, H., Nomura, M., 1988. Quantum efficiency of gold photocathodes (2–8 keV) and EXAFS in its secondary electron yield and in the detection currents of a microchannel plate and a silicon surface barrier detector. Rev. Sci. Inst. 59, 2453–2456.

Cromer, D.T., Liberman, D., 1970. Relativistic calculation of anomalous scattering factors for X-rays. J. Chem. Phys. 53, 1891–1898.

Elam, W.T., Kirkland, J.P., Neiser, R.R., Wolf, P.D., 1988. Depth dependence for extended X-ray-absorption fine-structure spectroscopy detected via electron yield in He and in vacuum. Phys. Rev. B38, 26–30.

El-Kareh, B., 1995. Fundamentals of Semiconductor Processing Technologies. Kluwer, Boston.

Gurman, S.J., 1983. An even simpler method for calculating X-ray absorption parameters. J. Phys. C16, 2987–3000.

Gurman, S.J., 1990. In: Hasnain, S. (Ed.), Synchrotron Radiation and Biophysics, (chap. 1). Ellis Horwood Ltd., Chichester, UK, pp. 10–42.

Henke, B.L., Knauer, J.P., Premaratne, J., 1981. The characterization of X-ray photocathodes in the 0.1–10-keV photon energy region. J. Appl. Phys. 52, 1509–1520.

Ohji, T., Sakai, S., Ito, M., Yamauchi, Y., Kanematsu, W., Ito, S., 1990. Fracture energy and tensile strength of silicon nitride at high temperatures. J. Ceram. Soc. Jpn Int. Ed. 98, 244–251.

Owens, A., 2002. XANES fingerprinting: a techniques for investigating CCD surface structures and measuring dead layer thicknesses, Nucl. Instrum. Methods, submitted for publication.

Owens, A., Fraser, G.W., Keay, A., Wells, A., McCarthy, K.J., Hill, H., Hughes, E.A., Smith, A.D., Suller, V., Surman, M., 1996. Mapping X-ray absorption fine structure in the quantum efficiency of an X-ray charge-coupled device. X-ray Spectrosc. 25, 33–38.

Owens, A., Denby, M., Wells, A., Keay, A., Graessle, D.E., Blake, R.L., 1997a. The effect of X-ray absorption fine structure in soft X-ray astronomical telescopes. Astrophys. J. 476, 924–932.

Owens, A., Bayliss, S., Fraser, G.W., Gurman, S.J., 1997b. On the relationship between total electron photoyield and X-ray absorption coefficient. Nucl. Instrum. Methods A358, 556–558.

Peterson, K.E., 1978. Dynamic micromechanisms on silicon: Techniques and devices. IEEE Trans. Electron. Devices ED-25 (10), 1241–1250.

Prigozhin, G.Y., Woo, J.W., Gregory, J.A., Loomis, A.H., Bautz, M.W., Ricker, G.R., Kraft, S., 1998. X-ray absorption near edge structure in the quantum efficiency of X-ray charge-coupled devices. Opt. Eng. 37, 2848–2854.

Roper, M., Buksh, P., Kirkman, I., van der Laan, G., Padmore, H., Smith, A., 1992. Performance of the Daresbury synchrotron radiation source soft X-ray double-crystal monochromator. Rev. Sci. Instrum. 63, 1322–1325.

Tatsumi, Y., Ohsaki, H., 1988. Density of crystalline and amorphous Si. In: Properties of Silicon, EMIS Datareviews Series Vol. 4. INSPEC, The Institution of Electrical Engineers, London, New York, pp. 3-6.

Veigele, W.J., 1973. Atom. Data Tables 5, 51–111.

Williams, G.P., 1986. Electron binding energies of the elements. In: Weast, R.C. (Ed.), CRC Handbook of Chemistry and Physics. 67th Edtion, CRC Press, Boca Raton, pp. F163–F166.